Available online at www.sciencedirect.com
ScienceDirect
Journal of Hazardous Materials 156 (2008) 421–427
Journal of Hazardous Materials
www.elsevier.com/locate/jhazmat

The reactor design and comparison of Fenton, electro-Fenton and photoelectro-Fenton processes for mineralization of benzene sulfonic acid (BSA)

Wang-Ping Ting [a], Ming-Chun Lu [b], Yao-Hui Huang [a,c,*]

[a] *Department of Chemical Engineering, National Cheng Kung University, Tainan 701, Taiwan*
[b] *Department of Environmental Resources Management, Chia Nan University of Pharmacy and Science, Tainan 717, Taiwan*
[c] *Sustainable Environment Research Center, National Cheng Kung University, Tainan 701, Taiwan*

Received 2 October 2007; received in revised form 10 December 2007; accepted 12 December 2007
Available online 23 December 2007

Abstract

A new approach for promoting ferric reduction efficiency using a different electrochemical cell and the photoelectro-Fenton process has been developed. The use of UVA light and electric current as electron donors can efficiently initiate the Fenton reaction. Benzene sulfonic acid (BSA) was the target compound in this study. The parameters investigated to evaluate the reactor design include the electrode working area, electrode distance, energy consumption. Furthermore, the study also contains the intermediates and the mineralization efficiency of electrolysis, Fenton, electro-Fenton and photoelectro-Fenton process.

Oxalic acid, the major intermediate of aromatic compound degradation, can complex with ferric ions. Meanwhile, a double cathode reactor could increase the current efficiency by 7%, which would translate to greater ferrous production and a higher degradation rate. Although the current efficiency of an electrode distance 5.5 cm device is 19% higher than 3.0 cm, results show that after 2 h of electrolysis the electronic expense using an electrode gap of 5.5 cm is much higher than 3.0 cm. The final TOC removal efficiency was 46, 64 and 72% using the Fenton, electro-Fenton and photoelectron-Fenton processes, respectively.

Keywords: Benzene sulfonic acid; Photoelectro-Fenton process; Current efficiency; Electrode distance; Energy consumption

1. Introduction

BSA is used mainly as an intermediate in the manufacture of azo dyestuffs, pharmaceuticals and tanning agents. Large amounts of aromatic sulfonated compounds have been produced as building blocks for the synthesis of dyes and detergents, and released into the environment as waste during their manufacture and use [1,2]. Aromatic sulfonated compounds are surface-active and very soluble in water. In contrast to the linear alkylbenzenesulfonates (LAS), which have been found to be readily biodegradable, other aromatic sulfonates without long alkyl side chains are reported to be persistent [3]. Consequently, it is difficult to remove them from water and they are transported from sewers to surface waters.

The Fenton reaction is a widely used and studied catalytic process based on an electron transfer between H_2O_2 and a metal acting as a homogeneous catalyst [4]. The reactivity of this system was first observed in 1894 by its inventor H. J. H. Fenton, but its utility was not recognized until the 1930s when a mechanism based on hydroxyl radicals was proposed [5]. The process may be applied to wastewaters, sludge, and contaminated soils to reduce toxicity, improve biodegradability, and remove odor and color [6–8]. During the Fenton process, hydrogen peroxide is catalyzed by ferrous ion to produce hydroxyl radicals [5].

$$Fe^{2+} + H_2O_2 \rightarrow Fe^{3+} + OH^- + {}^{\bullet}OH \quad (1)$$

This reaction is propagated from ferrous ion regeneration mainly by the reduction of the produced ferric species with

* Corresponding author at: Department of Chemical Engineering, National Cheng Kung University, Tainan 701, Taiwan. Tel.: +886 6 2757575x62636; fax: +886 6 2344496.
E-mail address: yhhuang@mail.ncku.edu.tw (Y.-H. Huang).

0304-3894/$ – see front matter © 2007 Elsevier B.V. All rights reserved.
doi:10.1016/j.jhazmat.2007.12.031

hydrogen peroxide [9],

$$H_2O_2 + Fe^{3+} \rightarrow Fe^{2+} + {}^{\bullet}H_2O + H^+ \quad (2)$$

However, in the Fenton chain reactions, the rate constant of Eq. (1) is between 53 and 76 $M^{-1}\,s^{-1}$ [5,10,11], while that of Eq. (2) is only 0.01 $M^{-1}\,s^{-1}$ [9]. This means ferrous ions are consumed more rapidly than they are produced. This results in the formation of a large amount of ferric hydroxide sludge during the neutralization stage of the Fenton process, which requires additional separation and disposal processes [12].

Recently, an electrochemical application method in the Fenton process, named the electro-Fenton method, has been reported in studies. These studies can be generally divided into four categories [6]. In type 1, hydrogen peroxide is externally applied while a sacrificial iron anode is used as a ferrous ion source [13–15]. In type 2, ferrous ion and hydrogen peroxide are electro-generated using a sacrificial anode and an oxygen sparging cathode, respectively [16]. In type 3, ferrous ion is externally applied, and hydrogen peroxide is generated by an oxygen sparging cathode [17,18]. In type 4, Fenton's regent was utilized to produce hydroxyl radical in the electrolytic cell, and ferrous ion was regenerated via the reduction of ferric ion on the cathode [19–21].

However, the electro-Fenton reaction still faces several obstacles that must be overcome first. The production of H_2O_2 is slow because oxygen has low solubility in water [22], and the current efficiency under pH 2.0 conditions is low [6]. This phenomenon is due to the formation of $Fe(OH)_3$ that is only slightly reduced to Fe^{2+} [12]. Stoichiometric electro-generated Fe^{2+} can be carried out at near neutral pH [23], thus overcoming the need for acidic conditions, which is a fundamental disadvantage of Fenton reactions in general. However, formation of ferric hydroxide sludge is still a problem here. The sludge can be electrochemically reduced to Fe^{2+}, but this requires a step in which the pH is lowered below 1 [12]. In principle the most promising electro-Fenton mode is type 4, in which the ferric ion is reduced to ferrous ion at the cathode. However, Fe^{2+} regeneration is slow even at an optimal current density.

More potent electro-Fenton methods with UV irradiation are also being developed for wastewater remediation, so-called photoelectro-Fenton process [24–27]. The process was irradiated with UVA light under electro-Fenton conditions. The action of this irradiation is complex and can be described by: (i) the production of greater amount of hydroxyl radical from photoreduction of $Fe(OH)^{2+}$, the predominant Fe^{3+} species in acid medium [6], by Eq. (3) and (ii) the photolysis of complexes of Fe(III) with generated carboxylic acids, as shown in Eq. (4) [6].

$$Fe(OH)^{2+} \xrightarrow{h\nu} Fe^{2+} + {}^{\bullet}OH \quad (3)$$

$$R(CO_2) - Fe(III) + h\nu \rightarrow R({}^{\bullet}CO_2) + Fe(II) \rightarrow {}^{\bullet}R + CO_2 \quad (4)$$

Oxalic acid is produced during the oxidation of most organics, and the fast photodecarboxylation of Fe(III)–oxalate complexes $Fe(C_2O_4)^+$, $Fe(C_2O_4)_2^-$, $Fe(C_2O_4)_3^-$ favors the decontamination process [6]. Under these conditions, it is also feasible to used sunlight as an alternative inexpensive source of UVA light using the solar photoelectro-Fenton process [24,28].

Therefore, in this study, we employed a novel photoelectro-Fenton method, in which Fenton's reagent was utilized to produce hydroxyl radical in the electrochemical cell and ferrous ion was regenerated via the reduction of ferric ion on the light source and cathode. The parameters investigated to evaluate the reactor design include the electrode working area, electrode distance, energy consumption. Furthermore, the study also contains the intermediates and the mineralization efficiency of electrolysis, Fenton, electro-Fenton and photoelectro-Fenton process.

2. Materials and methods

2.1. Chemicals and analytical method

All the reagents used in the experiments were in analytical quality (Merck). All the preparations and experiments were realized at the room temperature. The samples taken at predetermined time intervals were immediately injected into tubes containing sodium hydroxide solution to quench the reaction by increasing the pH to 11. The samples were then filtered with 0.45 μm, and kept for 12 h in the refrigerator before chemical oxygen demand (COD) analysis was conducted. This work has been carried out to correct quantitative the effect of the concentration of hydrogen peroxide on the COD value.

COD was determined using a closed-reflux titrimetric method based on Standard Methods [29]. The Fe^{2+} concentration was determined though titration with $KMnO_4$. TOC was determined with an Elementer (Germany)-liquid TOC total organic carbon analyzer. Organic acids were analyzed using Dionex DX-120 ion chromatograph with an IonPac® AS 11 anion column at 30 °C. The eluent concentration was generated by an RFIC eluent generation system. Technology follows Faraday's law ensures the accuracy of each eluent generation cartridge provided the applied current and eluent floe rate are accurately calibrated. Sample analysis with a RFIC system using a potassium hydroxide eluent gradient is the ideal choice to meet the separation and detection requirements of this application.

2.2. Experimental apparatus

Fig. 1 shows the schematic experimental setup of this study. The cylindrical reactor (radius: 6.5 cm and height: 35 cm) was operated at a constant current mode. The total volume of the reactor is 3.5 liters. The anode used is titanium net coated with RuO_2/IrO_2 (DSA), and the cathode is made of stainless steel. Three different cathode geometries were tested. Fig. 1(a) shows double electrode cell: with a inside diameter 7 cm DSA net as anode, 2 cm and 13 cm stainless steel wall as cathode; Fig. 1(b) shows single electrode cell: with a inside diameter 7 cm DSA net as anode and 13 cm stainless steel wall as cathode; Fig. 1(c) shows single electrode cell: with a inside diameter 2 cm DSA net as anode and 13 cm stainless steel wall as cathode.

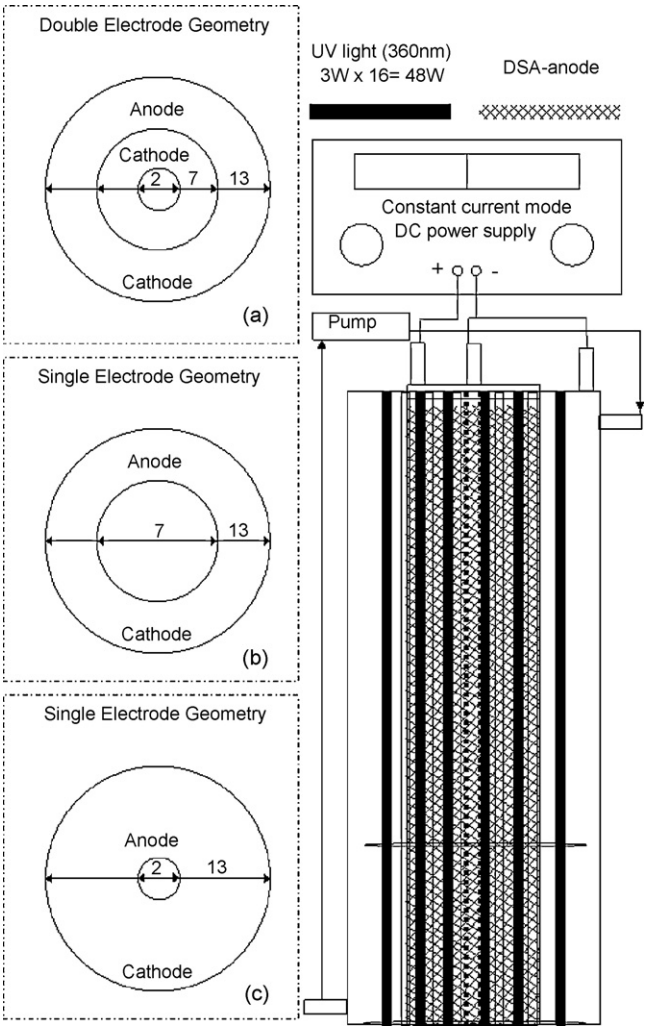

Fig. 1. (a–c) Schematic diagram of reaction system.

2.3. Electro-Fenton process

The reaction solution was poured into the system. The ferrous ion was added after the pH was adjusted to the desired value. The pH of the solution was not controlled during the reaction. In the meantime, hydrogen peroxide was added to the solution, and the power supply and the UVA source were turned on to initiate the reaction. The oxidation reaction was stopped instantly by adding NaOH to the reaction mixtures after sampling. The samples were then filtered with 0.45 μm to remove precipitates before analysis.

2.4. Photoelectro-Fenton process

The irradiation source was a set of sixteen 3 W UVA lamps (Sunbeamtech. com) fixed inside a cylindrical Pyrex tube (allowing wavelengths $\lambda > 320$ nm to penetrate). In addition to all the experimental conditions mentioned above, UV light with maximum wavelength of 360 nm was irradiated inside the reactor, supplying a photoionization energy input to the solution of 48 W.

3. Results and discussion

3.1. Performance of Fe^{2+} generation

The proposed reactions in the electrolytic system are [12]:

On the anode side:

$$H_2O \rightarrow 2H^+ + 1/2O_2 + 2e^- \quad (5)$$

$$Fe^{2+} \rightarrow Fe^{3+} + e^- \quad (6)$$

On the cathode side:

$$Fe^{3+} + e^- \rightarrow Fe^{2+} \quad (7)$$

$$H_2O + e^- \rightarrow 1/2H_2 + OH^- \quad (8)$$

The performance was evaluated by the instantaneous current efficiency (CE%) of ferrous ion generation, which is defined as [12]:

$$CE\,(\%) = \left(\frac{FV}{A}\right)\left(\frac{dC_{Fe}}{dt}\right) \times 100 \quad (9)$$

where F is Faraday's constant, C_{Fe} represents the concentration of generated ferrous ion, V is the volume of the solution, A is the operating current, and t is the reaction time. Since the current was kept constant, the amount of Fe^{2+} generated was proportional to the electrolysis time.

Fig. 2 shows the effect of cathode geometry (Fig. 1(a and b)) on the ferrous concentration generated, because the preferable reaction (Eq. (7)) occurred on the cathode. According to our past experience [12], a single working electrode does not significantly enhance the electro-regeneration of ferrous ion. For this reason, we developed a double cathode electrolysis cell (Fig. 1(a)) to increase the working area and to promote current efficiency. As shown in Eqs. (6) and (7), the small working area

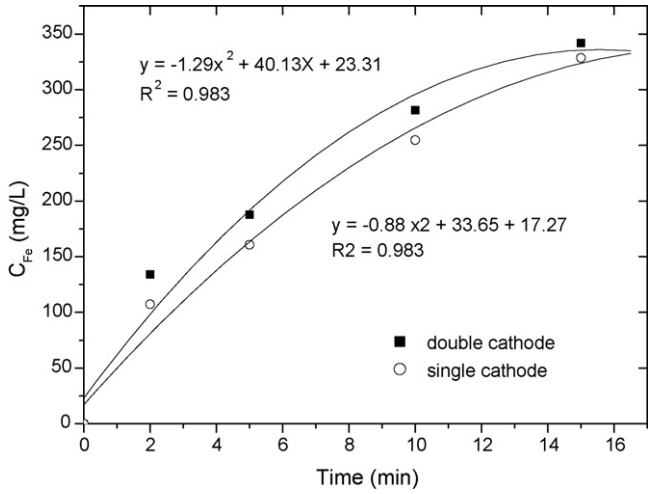

Fig. 2. Effect of cathode geometry on ferrous concentration. The solid line is the fit of second-order polynomial model ($Fe^{3+} = 1000$ mg/L; pH_i 2.0; $CD_a = 75.8$ A/m^2; (■): $CD_c = 71.0$ A/m^2, Fig. 1(a); (◯): $CD_c = 81.6$ A/m^2, Fig. 1(b), CD_a and CD_c denote the current densities of anode and cathode, respectively).

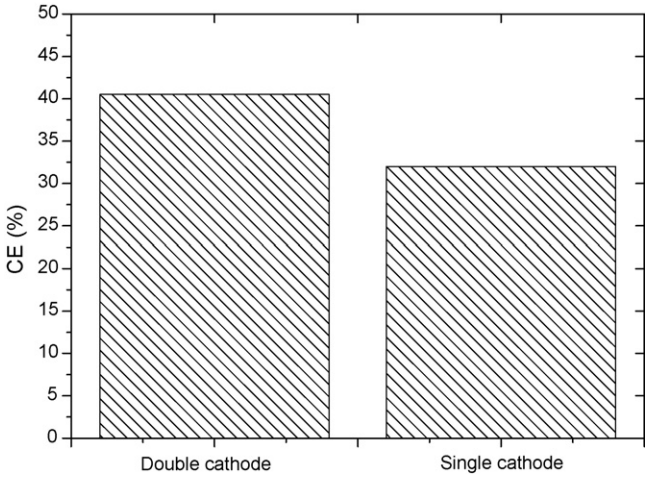

Fig. 3. Effect of cathode geometry on initial current efficiency (Fe^{3+} = 1000 mg/L; pH_i 2.0; CD_a = 75.8 A/m^2; double cathode reactor: CD_c = 71.0 A/m^2, Fig. 1(a); single cathode: CD_c = 81.6 A/m^2, Fig. 1(b)).

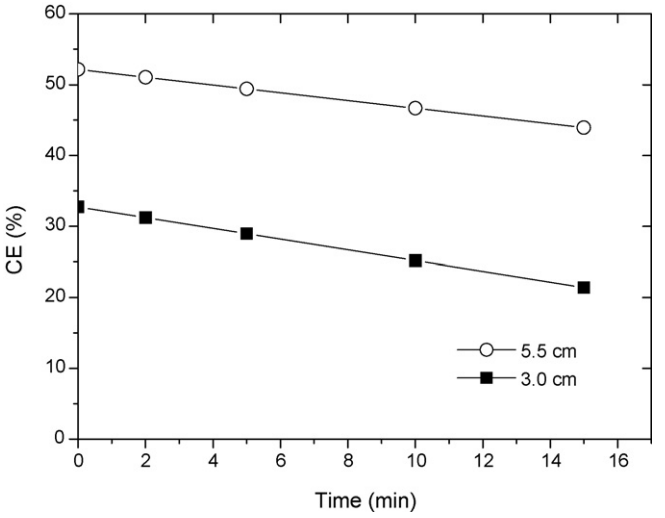

Fig. 4. Effect of electrode distance on current efficiency (Fe^{3+} = 1000 mg/L; pH_i 2.0; current = 10 A; single cathode reactor: 3.0 cm, Fig. 1(b); single cathode reactor: 5.5 cm, Fig. 1(c)).

on the anode was designed to minimize the oxidation of ferrous ion and to promote the reduction of ferric ion on the cathode. At the cathode, Fe^{3+} was electrochemically reduced to Fe^{2+} in an acidic solution. Simultaneously, H_2 evolution may occur as the side reaction which reduces the current efficiency. At the anode, the oxidation of H_2O leads to O_2 evolution and proton release. Consequently the ferrous concentration increased with increases in the cathode working area. Fig. 3 shows the effect of cathode geometry on initial current efficiency (Fig. 1(a and b)). The double cathode reactor could increase the current efficiency by 7%, which would translate to greater ferrous production and a higher degradation rate of organic compounds in the electro-Fenton process. A 41% current efficiency was observed using the double cathode electrochemical cell when CD_c = 71.0 A/m^2 and CD_a = 75.8 A/m^2. The CD_c and CD_a denote the current densities of the cathode and anode, respectively. Chou et al. reported that the initial current efficiency for Fe^{2+} regeneration was 39% at $[Fe^{3+}]_0$ = 1000 mg/L, CD_c = 98 A/m^2 and CD_a = 980 A/m^2 in the constant current mode [12]. It should be pointed out that the double cathode electrochemical cell has more potential for the improvement of the efficiency of electricity utilization.

Meanwhile the ferrous ion is oxidized to ferric ion on the anode by Eq. (6). Fe^{2+} regeneration is controlled either by the electron transfer between Fe^{3+} and the cathode or by the mass transfer of Fe^{3+} across the cathode–solution interface. Two geometries of electrode distance 3.0 and 5.5 cm (Fig. 1(b and c)) were employed to investigate the effect of electrode distance on Fe^{2+} regeneration. Fig. 4 shows the effect of electrode distance on current efficiency. A 52% current efficiency was observed in the trial using an electrode gap of 5.5 cm, and approximately 33% was detected in the trial using 3.0 cm. This shows a 19% increase in current efficiency which shows that long electrode distance can avoid the oxidation of ferrous ion on the anode.

3.2. Energy consumption with different electrode distances

To simplify the analysis, only electricity was considered. The energy consumption was calculated for electrode distances of 3.0 and 5.5 cm for the electro-Fenton process, respectively, when 1 kg COD needs to be removed. The energy cost for each device was obtained from Eq. (10).

$$\text{Energy consumption (kWh/kg COD)} = \frac{A\,\text{Voltage}\,t}{\Delta\text{COD}V} \quad (10)$$

$$\text{Resistance} = \frac{\text{Voltage}}{\text{Current}} \quad (11)$$

where A is the operating current, Voltage is the voltage, V is the volume of the solution, t is the reaction time and ΔCOD denotes the experimental COD decay in solution. The experimental results with regard to COD removal and energy consumption are shown in Table 1. Although the current efficiency of the 5.5 cm device is 19% higher than 3.0 cm, results show that after

Table 1
Effect of electrode distance on energy consumption ([BSA] = 10 mM; $[Fe^{2+}]$ = 8 mM; $[H_2O_2]_{overall}$ = 166 mM; pH_i 2.0; current = 10 A; H_2O_2 feeding time = 0, 5, 10, 15, 20, 30, 40, 60, 80, and 100 min; single cathode reactor: 3.0 cm, Fig. 1(b); 5.5 cm, Fig. 1(c))

Contact time (h)	Current (A)	Voltage (V)	Electrode distance (cm)	COD removal (%)	Energy consumption per kg COD removal (kWh/kg COD)
0.5	9.99	8.1	3.0	50	12.58
1	9.99	7.2	3.0	63	17.60
2	9.99	6.9	3.0	71	28.35
0.5	10.00	19.6	5.5	55	26.59
1	10.00	16.8	5.5	66	38.53
2	9.99	16.5	5.5	74	62.59

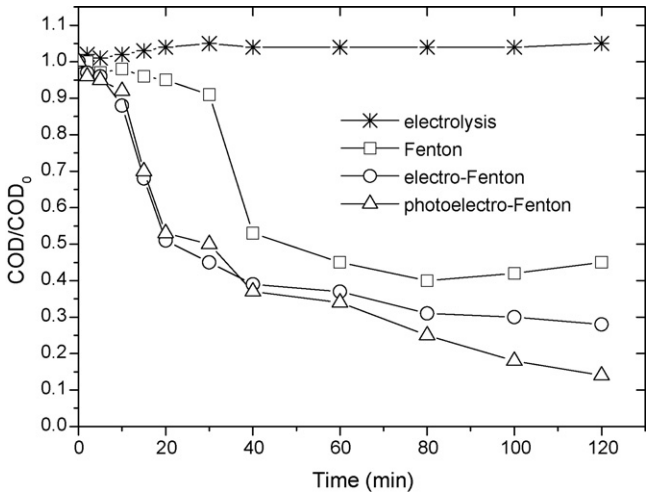

Fig. 5. Effect of different processes on COD removal efficiency ([BSA] = 10 mM; $[Fe^{2+}]$ = 8 mM; $[H_2O_2]_{overall}$ = 166 mM; pH_i 2.0; CD_a = 75.8 A/m^2; CD_c = 71.0 A/m^2; H_2O_2 feeding time = 0, 5, 10, 15, 20, 30, 40, 60, 80, and 100 min).

2 h of electrolysis the electronic expense using an electrode gap of 5.5 cm is much higher than 3.0 cm. The result suggests that the electrode distance 3.0 cm device can provide more economical operation.

This phenomenon is due to Eq. (11). Long electrode distance will enhance the resistance causing the voltage and electricity cost to be higher. The results were compared with the results obtained by Brillas and Casado, when aniline was treated with Ti/Pt anode and carbon-PTFE cathode [16]. The electro-Fenton process used by Brillas has a higher energy cost (45 kWh m^{-3} for 2 h) than this system (39 kWh m^{-3} at 2 h, the data calculated from 3.0 cm device: Fig. 1(b)).

3.3. Degradation of BSA in different processes

Based on the results of current efficiency and energy consumption, the double cathode device (Fig. 1(a)) should be used for further oxidation research. Electrolysis, Fenton, electro-Fenton and photoelectron-Fenton experiments were conducted to investigate the synergistic effect of combined photo and electrochemical methods. Fig. 5 showed that the electrochemical method could hardly remove COD from the BSA solution. In this method, hydroxyl radicals would be produced at the surface of a high-oxygen overvoltage anode from water oxidation.

$$H_2O \rightarrow {}^{\bullet}OH + H^+ + e^- \quad (12)$$

However, electrolysis did not oxidize with time since the overvoltage of DSA anode is not enough for amount of $^{\bullet}$OH gendered. The same tendency can be finding in the research of Zhang at al [19].

In the electro-Fenton process, COD was removed rapidly during the first 20 min. The final COD removal efficiency achieved by the electro-Fenton process was nearly 17% higher than that of the Fenton's reagent alone. Meanwhile, the photoelectron-Fenton process achieved a COD removal efficiency that was 14% higher than that of the electro-Fenton process. This indicated that the photoelectro-Fenton method had synergistic effect for COD removal.

3.4. Effect of different processes on mineralization and intermediate products

To investigate the synergistic effect of combined irradiation, electrochemical method and Fenton's reagent, 720 mg/L TOC of BSA solution was treated with Fenton reagent alone, the electro-Fenton method alone and the photoelectro-Fenton method, respectively. Fig. 6 shows that the Fenton process could only slightly remove TOC from the BSA solution. Furthermore in both the electro-Fenton and the photoelectro-Fenton processes, TOC was removed faster during the first hour. After that, only slow changes in TOC were observed because ferric ion was complexed by oxidation products such as oxalic acid. The degradation of aromatic compounds often leads to the formation of intermediates such as glyoxylic, maleic, oxalic, acetic and formic acids [6,30]. Fig. 7 indicates the formation of oxalate acid and formic acid. Oxalate acid would be reduced from the electro-Fenton and photoelectro-Fenton processes. As result of Fig. 7, the ferric complexes would be reduced to ferrous ion from the photo-reduction and by reduction in the cathode. This would induce the Fenton chain reaction efficiently.

As shown in Eq. (4), the photo-reactivity of Fe(III)–carboxylate or Fe(III)–polycarboxylate complexes usually leads to decarboxylation of the organic ligand [6,31]. The use of UVA light and electric current as electron donors can efficiently initiate the Fenton reaction. Oxalic acid, the major intermediate of aromatic compound degradation, can complex with ferric ions. These complexes typically have higher molar absorption coefficients up to 500 nm in the near-UV and visible regions leading to the generation of ferrous ion [4]. Meanwhile, the ferrous ion is regenerated via the reduction of ferric ion on the cathode.

The photochemistry of Fe^{3+} is advantageous to the Fenton process because the reduced iron can react with H_2O_2 to

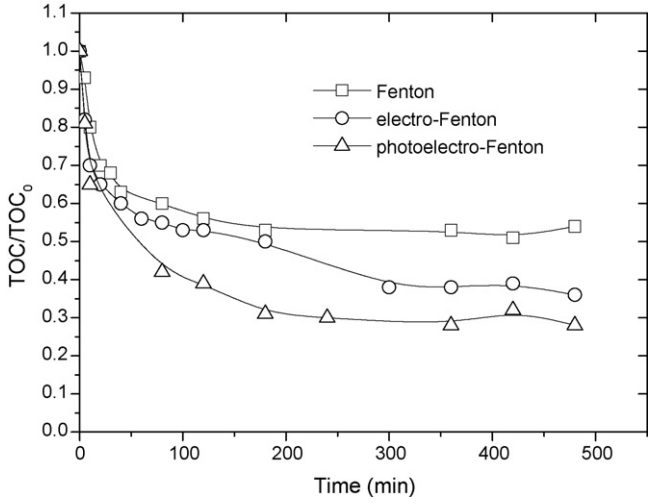

Fig. 6. Mineralization of BSA with different processes. ([BSA] = 10 mM; $[Fe^{2+}]$ = 8 mM; $[H_2O_2]$ = 166 mM; pH_i 2.0; CD_a = 75.8 A/m^2; CD_c = 71.0 A/m^2).

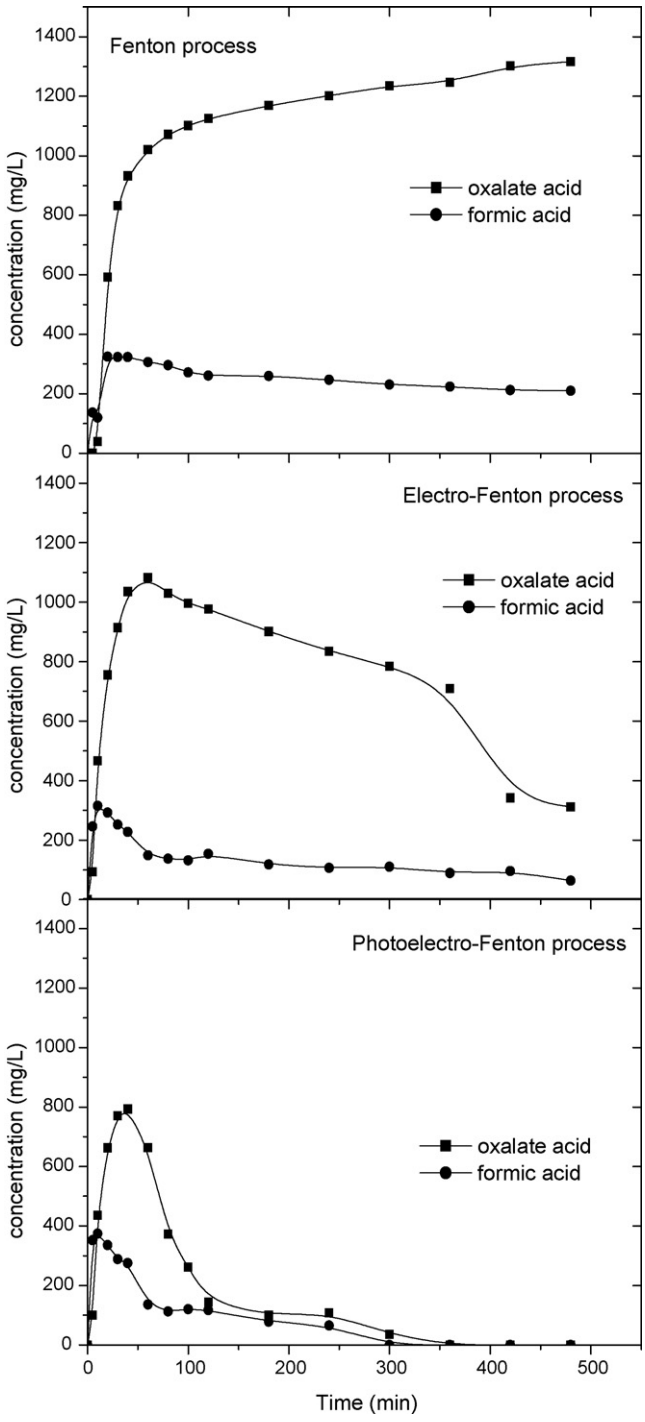

Fig. 7. Formation of organic acid by the degradation of BSA ([BSA] = 10 mM; $[Fe^{2+}]$ = 8 mM; $[H_2O_2]$ = 166 mM; pH_i 2.0; CD_a = 75.8 A/m^2; CD_c = 71.0 A/m^2).

produce •HO. The final TOC removal efficiency achieved by the electro-Fenton method was 64%, nearly 20% higher than Fenton's reagent alone. Meanwhile, the final TOC removal efficiency achieved by the photoelectro-Fenton method was 72%. This indicates that irradiation and electrochemical methods had a synergistic effect for TOC removal because the photoelectro-Fenton reaction takes advantage of the photo-reduction of Fe(III)–oxalate complexes [6]. Bolton and coworkers added oxalate to the reaction solution and observed the photoreduction of the resulting ferrioxalate complexes, such as

$$[Fe(C_2O_4)_3]^{3-} \xrightarrow{h\nu} Fe^{2+} + 2C_2O_4^{2-} + {}^{\bullet}C_2O_4^{-} \quad (13)$$

and obtained degradation of aromatic and chlorinate aromatic hydrocarbons [4]. However, photodecomposition of Fe^{3+} complexes produced some short organic acids, which are produced in the last degradation steps before total conversion to CO_2 [32]. This is especially relevant with regard to the oxalic acid mineralization. The ferric complexes would be reduced to ferrous ion from the photo-reduction and by reduction in the cathode. This would induce the Fenton chain reaction efficiently.

4. Conclusion

The effect of electrode geometry and different oxidation methods were investigated to evaluate reactor design and mineralization efficiency. The double cathode reactor could increase the working area and enhance the current efficiency by 7%, which would translate to greater ferrous production and a higher degradation rate of organic compounds in the electro-Fenton process. It should be pointed out that the double cathode electrochemical cell has more potential for the improvement of the efficiency of electricity utilization. The result also suggests that the electrode distance 3.0 cm device can provide more economical operation. The final COD removal efficiency achieved by the electro-Fenton process was 17% higher than that using the Fenton's reagent alone. Meanwhile, the photoelectro-Fenton process achieved a COD removal efficiency that was 14% higher than that of the electro-Fenton process. The same tendency was shown in the TOC removal. This indicates that the photoelectro-Fenton method had a synergistic effect for mineralization. Oxalic acid, the major intermediate of aromatic compound degradation, can complex with ferric ions. The ferric complexes would be reduced to ferrous ion from photo-reduction and by reduction in the cathode. This would induce the Fenton chain reaction efficiently.

Acknowledgement

The authors would like to thank the National Science Council of Taiwan, Republic of China, for financially supporting this research under Contract No. NSC96-2628-E-041-002-MY3.

References

[1] M. Takeo, T. Nagayama, K. Takatani, Y. Maeda, M. Nakaoka, Mineralization and desulfonation of 3-nitrobenzenesulfonic acid by alcaligenes sp. GA-1, J. Ferment. Bioeng. 83 (1997) 505–509.
[2] M.C. Alonso, L. Tirapu, A. Ginebreda, D. Barcelo, Monitoring and toxicity of sulfonated derivatives of benzene and naphthalene in municipal sewage treatment plants, Environ. Pollut. 137 (2005) 253–262.
[3] H. Takada, R. Ishiwatari, Biodegradation experiments of linear alkylbenzenes (LABs): isomeric composition LABs as an indicator of the degree of LAB degradation in the aquatic environment, Environ. Sci. Technol. 24 (1990) 86–91.
[4] A. Safarzadeh-Amiri, J.R. Bolten, S.R. Cater, The use of iron in advanced oxidation processes, J. Adv. Oxid. Technol. 1 (1996) 18–26.

[5] C. Walling, Fenton's reagent revisited, Acc. Chem. Res. 8 (1975) 121–131.
[6] J.J. Pignatello, E. Oliveros, A. Mackay, Advanced oxidation processes for organic contaminant destruction based on the Fenton reaction and related chemistry, Crit. Rev. Env. Sci. Technol. 36 (2006) 1–84.
[7] M.C. Lu, C.J. Lin, C.H. Liao, W.P. Ting, R.Y. Hiang, Influence of pH on the dewatering of activated sludge by Fenton's reagent, Water Sci. Technol. 44 (2001) 327–332.
[8] M.C. Lu, C.J. Lin, C.H. Liao, R.Y. Hiang, W.P. Ting, Dewatering of activated sludge by Fenton's reagent, Adv. Environ. Res. 7 (2003) 667–670.
[9] C. Walling, Mechanism of the ferric ion catalyzed decomposition of hydrogen peroxide: effects of organic substrate, J. Am. Chem. Soc. 95 (1973) 2987–2991.
[10] T. Rigg, W. Taylor, J. Weiss, The rate constant of the reaction between hydrogen peroxide and ferrous ions, J. Chem. Phys. 22 (1954) 575–577.
[11] D.I. Metelitsa, Mechanisms of the hydroxylation of aromatic compounds, Russ. Chem. Rev. 40 (1971) 563–580.
[12] S. Chou, Y.-H. Huang, S.-N. Lee, G.-H. Huang, C. Huang, Treatment of high strength hexamine-containing wastewater by electro-Fenton method, Water Res. 33 (1999) 751–759.
[13] N. Kannan, G. Karthikeyan, N. Tamilselvan, Comparison of treatment potential of electrocoagulation of distillery effluent with and without activated *Areca catechu* nut carbon, J. Hazard. Mater. 137 (2006) 1803–1809.
[14] I.A. Sengil, M. ozacar, Treatment of dairy wastewaters by electrocoagulation using mild steel electrodes, J. Hazard. Mater. 137 (2006) 1197–1205.
[15] U. Kurt, O. Apaydin, M.T. Gonullu, Reduction of COD in wastewater from an organized tannery industrial region by electro-Fenton process, J. Hazard. Mater. 143 (2007) 33–40.
[16] E. Brillas, J. Casado, Aniline degradation by Electro-Fenton$^{(R)}$ and peroxi-coagulation processes using a flow reactor for wastewater treatment, Chemosphere 47 (2002) 241–248.
[17] C. Badellino, C.A. Rodrigues, R. Bertazzoli, Oxidation of pesticides by in situ electrogenerated hydrogen peroxide: Study for the degradation of 2,4-dichlorophenoxyacetic acid, J. Hazard. Mater. 137 (2006) 856–864.
[18] E. Kusvuran, S. Irmak, H.I. Yavuz, A. Samil, O. Erbatur, Comparison of the treatment methods efficiency for decolorization and mineralization of Reactive Black 5 azo dye, J. Hazard. Mater. 119 (2005) 109–116.
[19] H. Zhang, C. Fei, D. Zhang, F. Tang, Degradation of 4-nitrophenol in aqueous medium by electro-Fenton method, J. Hazard. Mater. 145 (2007) 227–232.
[20] C.-W. Li, Y.-M. Chen, Y.-C. Chiou, C.-K. Liu, Dye wastewater treated by Fenton process with ferrous ions electrolytically generated from iron-containing sludge, J. Hazard. Mater. 144 (2007) 570–576.
[21] H. Zhang, D. Zhang, J. Zhou, Removal of COD from landfill leachate by electro-Fenton method, J. Hazard. Mater. 135 (2006) 106–111.
[22] A. Savall, Electrochemical treatment of industrial organic effluents, Chimia 49 (1995) 23–27.
[23] K. Pratap, A.T. Lemley, Fenton electrochemical treatment of aqueous atrazine and metolachlor, J. Agric. Food Chem. 46 (1998) 3285–3291.
[24] C. Flox, J.A. Garrido, R.M. Rodríguez, P.L. Cabot, F. Centellas, C. Arias, E. Brillas, Mineralization of herbicide mecoprop by photoelectro-Fenton with UVA and solar light, Catal. Today 129 (2007) 29–36.
[25] I. Sirés, C. Arias, P.L. Cabot, F. Centellas, J.A. Garrido, R.M. Rodríguez, E. Brillas, Degradation of clofibric acid in acidic aqueous medium by electro-Fenton and photoelectro-Fenton, Chemosphere 66 (2007) 1660–1669.
[26] B. Boye, M.M. Dieng, E. Brillas, Degradation of herbicide 4-chlorophenoxyacetic acid by advanced electrochemical oxidation methods, Environ. Sci. Technol. 36 (2002) 3030–3035.
[27] E. Brillas, J.C. Calpe, J. Casado, Mineralization of 2,4-D by advanced electrochemical oxidation processes, Water Res. 34 (2000) 2253–2262.
[28] J. Casado, J. Fornaguera, M.I. Galán, Mineralization of aromatics in water by sunlight-assisted electro-Fenton technology in a pilot reactor, Environ. Sci. Technol. 39 (2005) 1843–1847.
[29] APHA, Standard Methods for the Examination of Water and Wastewater, 20th ed., American Public Health Association, Washington, DC, USA, 1998.
[30] E. Brillas, E. Mur, R. Sauleda, L. Sanchez, J. Peral, X. Domenech, J. Casado, Aniline mineralization by AOP's: anodic oxidation, photocatalysis, electro-Fenton and photoelectro-Fenton processes, Appl. Catal. B: Environ. 16 (1998) 31–42.
[31] V. Balzani, V. Carassiti, Photochemistry of Coordination Compounds, Academic Press, New York, 1970.
[32] E. Exposito, C.M. Sanchez-Sanchez, V. Montiel, Mineral iron oxides as iron source in electro-Fenton and photoelectro-Fenton mineralization processes, J. Electrochem. Soc. 154 (2007) E116–E122.